

Computer Vision and Pattern Recognition - Coursework 2

Name: Krithika Balaji, Username: KB4317, CID: 01378251

Name: María de la Paz Cardona Sánchez, Username: MDC5017, CID: 01410045

Refer appendices A-D for figures in sections A-D.

Section A: Data Preparation

Part 1 Three different objects were chosen: kitchen sponge, flour sack and steel vase. The PVT and Electrodes data of these objects was plotted (Fig. 1, 2 and 3). Data plotted corresponds to finger F0, arbitrarily chosen after verifying that there was no significant difference in the F0 and F1 plots, since both fingers contain the same sensors.

Intuitively, for the choice of time instant, an ideal point would be that when the sensor is already touching the object but still in the first instants so that deformable soft objects are not presenting any resistance. In theory, this point would give different parameters for objects of different nature (deformable vs non-deformable).

By qualitatively looking at the plots, time step $t=50$ showed enough variability across the objects. To quantitatively verify that $t=50$ was an appropriate point, the variance between the different objects of the mean trial values for these parameters was calculated. Although $t=999$ was the point with the highest variance for pressure and temperature, and $t=1$ was the point with the highest variance for vibration, these were discarded because they were points at the very start of the movement or at the very end. $t=50$ showed a high variance value within the same order of magnitude of the highest variance, confirming it was an appropriate point. Variance values can be found in Appendix A, Table 1.

Part 2 For F0, the sampled values at time $t = 50$ for each object and trial were stored into a .mat containing 2 matrices: sampledDataECon and sampledDataPVTCon. Detailed description can be found in Appendix A, Part 2.

Part 3 Fig. 4 contains a 3D scatter plot of the complete contents of the PVT mat file.

Section B: Prin. Component Analysis

Part 1a Covariance matrix, eigenvalues and eigenvectors can be found in Appendix B, Part 1a.

Part 1b Fig. 5 shows the standardised data with the principal components i.e the eigenvectors from Part 1a.

Part 1c The two principal components correspond to the two eigenvectors with highest eigenvalue (col. 2 and 3 from V matrix). Data reduced to 2D is shown in Fig. 6.

Part 1d Fig. 7 shows data distributed across all principal components individually.

Part 1e In Fig. 6 data was reduced to 2D (using `biplot()`) and still keeps enough information to mostly tell objects apart. There are some points where the black foam, car sponge and flour sack values are slightly mixed up (especially the two sponges). Given that these are soft deformable objects with similar properties it makes sense that it can be difficult to tell them apart just by touch. The steel vase and acrylic points are completely mixed up - these two can be classified as hard and non-deformable and from Fig. 5, they seem to have similar PVT properties. PCA does provide a clear separation between soft and hard objects that can be seen in 2D (Fig. 5) but also in 1D on the first principal component (Fig. 9 left).

Part 2a Fig. 8 contains a scree plot showing the variances of each principal component of the electrode data.

Part 2b After a dimensionality reduction (from 19D to 3D), electrode data maintains enough information to mostly tell objects apart (Fig. 9), with some exceptions. Distinction between soft and hard can be easily achieved.

Part 2c With the electrode data it is possible to clearly tell apart between black foam, flour sack and car sponge, which the PCA of the PVT mixed up slightly. But kitchen sponge, which was clearly identified after PCA of the PVT, is now mixed up with the flour sack. Hard objects (acrylic and steel vase) are difficult to tell apart. For a better classification result, it would be best to use all of the parameters available. However, PVT could suffice for just distinguishing between soft and hard. Fig. 8 confirms that the minimum number of dimensions that should be kept for the electrode data is 3,

reducing to 2D or 1D would translate in a significant loss of information from which correct object classification would be very difficult to achieve.

Section C: Linear Discriminant Analysis

Part 1a LDA was used to split the data for black foam and car sponge in terms of Pressure vs Vibration (Fig. 10), Pressure vs Temperature (Fig. 11) and Temperature vs Vibration (Fig. 12).

Part 1b LDA was applied on the 3D PVT data for black foam and car sponge. Fig. 13 shows the data projected onto 1D and 2D. Fig. 14 shows the two main linear determinants in relation to the 3D PVT data.

Part 1c In Fig. 13, clear class separation can be seen between car sponge and black foam, as there is a visible gap at around 0 between the two classes.

In contrast, while the classes have clearly been separated in Fig. 10, 11 and 12, there is not a significant gap between the two classes, suggesting good class separation requires consideration of all PVT parameters. This could be due to both objects having similar surface textures, resulting in similar vibrations being detected. This is supported by Fig. 12, where the LD vector has a steep, downward gradient. This suggests there is not much separation to be done based on vibration while temperature proves a more suitable comparative dimension. This can also be seen in Fig. 10 - while the graph is not as steep as in Fig. 12, it is still steep enough that pressure clearly proves a more suitable dimension for class separation. This reduction in steepness could be due to the fact that both objects deform under pressure. Similar physical properties could also be why there is imperfect class separation in the numberlines (Fig. 10, 11 and 12) [1].

Part 1d The above analyses were repeated for the kitchen sponge and steel vase data to test whether similar physical properties lead to lower cluster separability. These objects have different physical properties. The sponge is rough to touch, while the vase is smooth, resulting in varied vibrations. While the sponge deforms under pressure, the vase does not, resulting in varied pressure data. LD profiles can be seen in Fig. 15, 16 and 17. The 3D scatter plot of the PVT data for these two objects and the LDA analysis can be seen in Fig. 18 and 19 respectively.

From Fig. 16 and 17, it seems like both objects have similar temperature ranges, as the LD axes are nearly vertical and horizontal respectively, suggesting that minimal class separation can be done based on temperature.

The two objects seemingly respond differently to pressure and vibration. The hypothesis of varying surfaces of the two objects affecting vibration is supported in Fig. 17, where the LD line is near horizontal. This suggests that class separation can only reliably be done based on vibration. The hypothesis of varying deformation capabilities under pressure is also supported in Fig. 16, where the LD line is near vertical. This suggests that class separation can only reliably be done based on pressure.

In Fig. 16, two sub-clusters can be seen within the steel vase cluster. A possible explanation is that, between trials, the vase might have been moved by the robot. Assuming a circular cross-section across which the fingers will hold the vase, the pressure felt by the sensors could vary depending on whether the vase is held securely across its cross-sectional diameter or if it is held a few centimeters away from the diameter, leading to two groups of pressure values.

Class separation seems perfect - all the kitchen sponge points and the steel vase points are grouped together with no mixing (Fig. 19). This could be due to the differences in physical properties of the materials being distinct for kitchen sponge and steel vase.

Section D: Clustering

Part 1a K-means output is shown in Fig. 20.

Part 1b Algorithm performance depends on similarity of the objects to be classified. Some black foam data points have been assigned to the car sponge cluster and one car sponge point has been labelled as black foam. These misclassifications could be due to their similar PVT properties and the fact that they both are sponges. This confusion between the sponges types also occurred when performing PCA - after reducing PVT data to 2D there was not a clear separation between these objects. Steel vase and acrylic points (both hard and non-deformable objects) are spread out in two different clusters. Their PVT properties do not seem to be unique enough for perfect clustering. Flour sack and kitchen sponge were classified in clusters of their own without any misclassification.

Part 1c K-means was repeated using correlation distance (Fig. 21). The definition of this metric can be found in Appendix D, Part 1c. Here, there is more misclassification between car sponge, black foam and flour sack (all soft, deformable objects). Steel vase and acrylic are spread out in three different clusters. All the kitchen sponge points are classified in their own cluster with no errors.

Part 2a 30 trees were chosen for the bagging algorithm. This was reduced from a 150 trees, where it was

seen that the Out-of-Bag (OOB) Classification error started to plateau at around 30 trees at an error of ~ 0.17 (Fig. 22). Any further decreases to the OOB classification error from increasing the number of trees would increase computations and possibly run the risk of overfitting to the training data, which would lead to poorer generalizations when tested on unseen data.

Part 2b Fig. 23 and 24 are visualizations of two of the generated decision trees out of 30.

Part 2c Fig. 25 displays the confusion matrix. The model accuracy is 83.3% - only 4 out of the 24 test data were misclassified. This is a fairly high accuracy.

Part 2d The main error is in classifying acrylic as steel vase. Both are hard objects that do not deform under pressure and hence are likely to have similar pressure values picked up by the 19 electrodes. It seems likely that there is a bias towards steel vase data for harder objects, seeing as all the steel vase data were classified correctly as being steel vase while all the acrylic data were classified incorrectly as being steel vase as well. PCA helped in data dimensionality reduction from 19 to 3 dimensions, hence reducing the number of computations needed. When initially using the 19 PCA dimensions, the OOB error plateaued at around 50 bags (See Fig. 26) at an error of 0.3. With 3 dimensions, however, the OOB plateaued at 30 bags at an error of 0.17, allowing for less computations to be performed along with lower error.

Section E: Conclusion

Part 1a PCA helped reduce the dimensionality of the PVT/electrode data and projected the data onto 2D and 3D respectively, to make it easier to understand and visualize. It was found that the maximum variance was along axes that were a combination of the three PVT properties.

LDA helped reduce data dimensionality by choosing axes that allowed for the greatest class separability. This helped in analysing the similarities and differences in physical properties between pairs of objects, using pressure, vibration and temperature. Depending on how different the objects were with respect to two of the PVT variables, class separation was more distinct. The LD lines' slope when reducing 2D graphs to 1D also gave insights into how similar or different objects were for different properties.

K-means achieved an overall satisfactory classification of the different objects, with some misclassifications between the sponges and between the acrylic and the steel vase. It did, however, outstandingly at more general classification of hard vs soft objects. Bagging trained a model that could

classify objects based on their dimensionality-reduced electrode data. It also achieved fine classification, with the only errors being in classifying acrylic. The model can now predict the class given any new PCA-reduced electrode data.

Part 1b General object categories can be determined based on touch but it would be harder to determine the exact object within the same group due to similar physical properties. For instance, in Section C, when kitchen sponge and steel vase were paired for LDA, clear separability could be seen between the two classes due to the differences in physical properties. When black foam and car sponge were paired, however, class separability was not as clear due to the similar physical properties. Bagging generally had high accuracy but could not distinguish between hard objects, just as K-means. So while deformable versus hard objects could be distinguished, the exact objects could not when the pair of objects had similar properties and nature.

Part 1c The most relevant object properties seem to depend on the analysis method chosen and the object types that are being compared. LDA shows that temperature did not play a huge role for object pairs that were very distinct from each other. In contrast, pressure and vibration played a significant role, as they provided information on how deformable an object is and its texture respectively. For separation of the given object categories, it would suffice to use only pressure and vibration data, as there seems to not be great temperature variations between classes. For more accurate separations, all three would be necessary as temperature could potentially provide extra information that could help hone in on the exact object. One could also consider discarding PVT data and only using electrode data, seeing as bagging generally achieved high classification accuracy. Experimentation can also be done with less electrodes to see how that affects accuracy.

Part 1d An alternative method for data preparation is to average the data for each trial and for each object across a small time window. This would help find the central tendency of the pressure, vibration, temperature and electrodes data over a window, instead of at a single point. The advantages are that this is fast and easy to calculate and we would be considering more of the values collected at each trial over time in our analyses. The disadvantage is this method works only when all values are equally important and you are assuming there are no errors or big movements. If the data, however, is collected from the middle of the temporal series, this should not be a significant problem as it is unlikely that the robot will make big movements before the 'hold' position is programmed to end.

References

- [1] ElastoProxy. Foam Rubber vs. Sponge Rubber: What's the Difference?. <https://www.elastoproxy.com/foam-rubber-vs-sponge-rubber/> Viewed 8 Mar 2021.
- [2] MathWorks. K-means - input arguments 'Distance'. <https://uk.mathworks.com/help/stats/kmeans.html#buefs04-Distance> Viewed 8 Mar 2021.

1. Appendices

Appendix A

Run section_a.m to obtain the images below.

Part 1

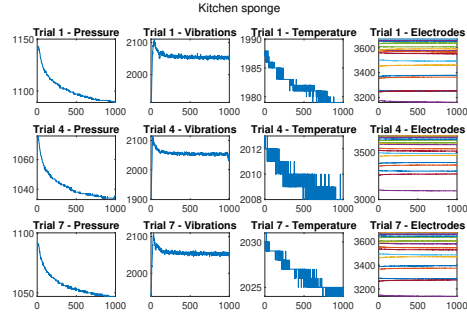


Figure 1: Kitchen sponge data for different trials.

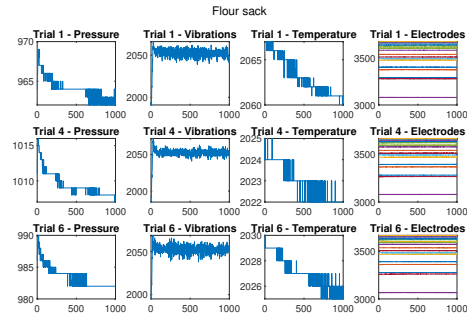


Figure 2: Flour sack data for different trials.

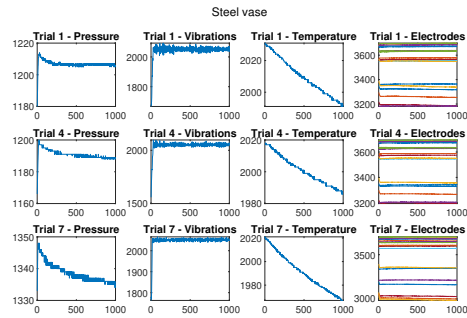


Figure 3: Steel vase data for different trials.

Variance Values

	t=1	t = 50	t = 999
Pressure	1.1128e+04	1.2968e+04	1.4072e+04
Vibrations	1.5535e+04	196.9550	5.7070
Temperature	1.0479e+03	1.0807e+03	1.8768e+03

Table 1: Variance values.

Part 2

F0_PVT_V6_t50.mat contains all the data structures this question asked for. sampledDataECon is of size 20x60 where the first dimension contains information on the electrode number. The second matrix is of size 4x60, where the first dimension contains information on pressure, vibration and temperature respectively. For both matrices, the second dimension contains

information on every trial for each object and the first rows are object labels from 1-6 in the following order: acrylic, black foam, car sponge, flour sack, kitchen sponge and steel vase.

Part 3

Figure 4 shows the 3D scatter plot of the raw PVT data.

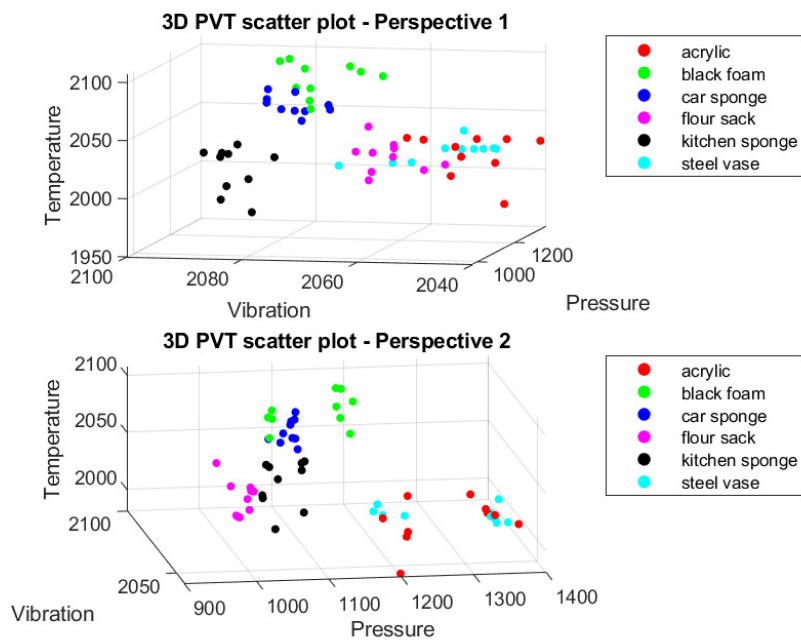


Figure 4: 3D scatter plot of the entire PVT data.

Appendix B

Run section_b.m to obtain the images below.

Part 1a After normalising the data using `zscore()`, covariance matrix was found to be:

$$C = \begin{pmatrix} 1 & -0.3568 & -0.3185 \\ -0.3568 & 1 & 0.2693 \\ -0.3185 & 0.2693 & 1 \end{pmatrix} \quad (1)$$

The eigenvalues of C were:

$$D = \begin{pmatrix} 0.6337 & 0 & 0 \\ 0 & 0.7352 & 0 \\ 0 & 0 & 1.6311 \end{pmatrix} \quad (2)$$

and its eigenvectors:

$$V = \begin{pmatrix} 0.7803 & -0.1630 & -0.6038 \\ 0.5685 & 0.5870 & 0.5764 \\ 0.2605 & -0.7930 & 0.5507 \end{pmatrix} \quad (3)$$

Part 1b

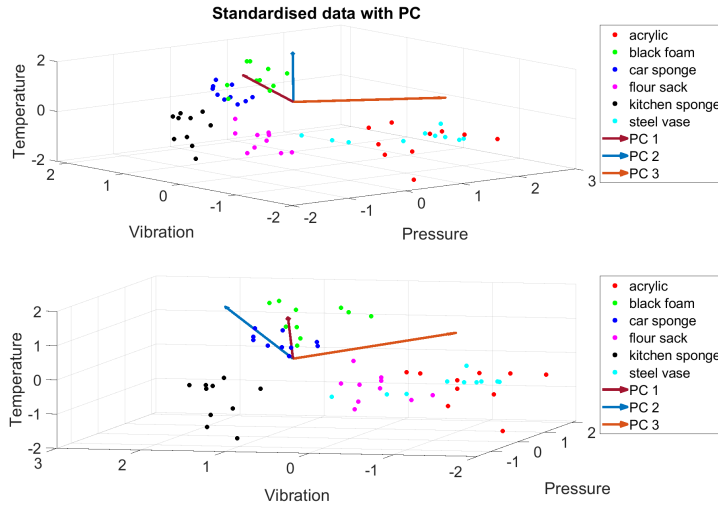


Figure 5: Standardised data with PCA components displayed.

Part 1c

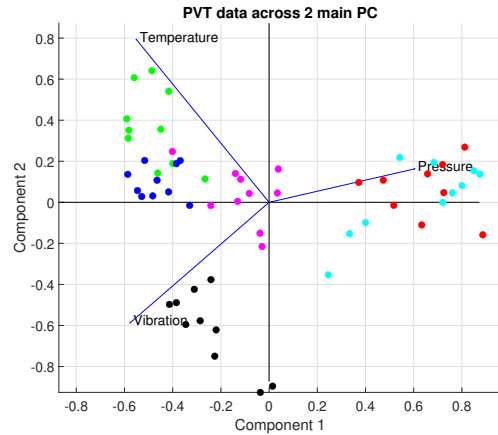


Figure 6: PVT data reduced to 2D.

Part 1d

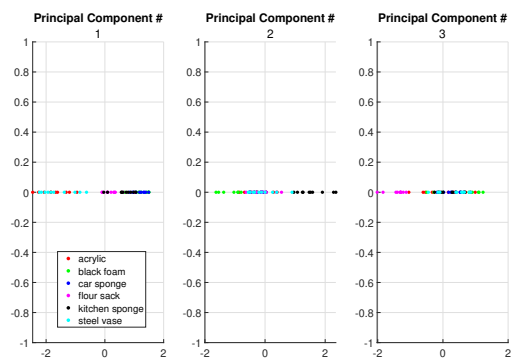


Figure 7: PVT data across all principal components.

Part 2a

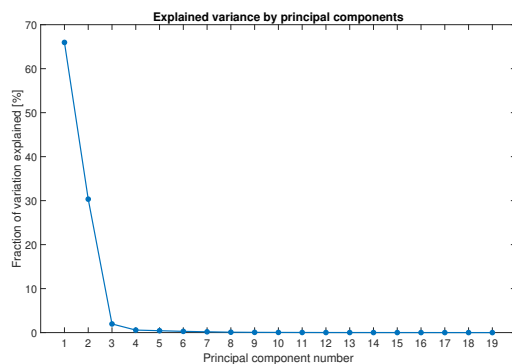


Figure 8: Scree plot of electrode data.

Part 2b

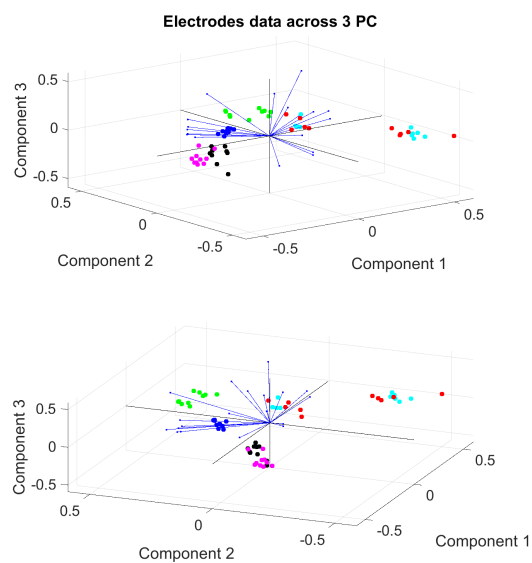


Figure 9: Electrode data across 3 main principal components.

Appendix C

Run section_c.m to obtain these images.

Part 1a

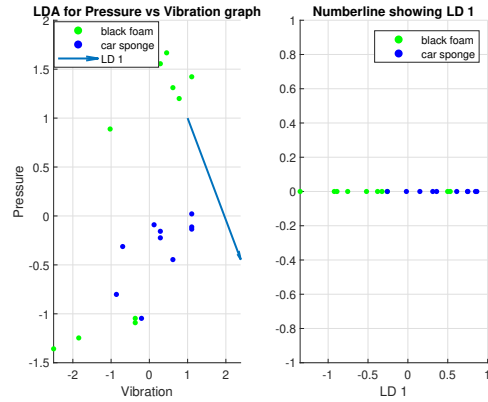


Figure 10: 2D scatter plot of Pressure vs Vibration for black foam and car sponge along with the dimension reduced data.

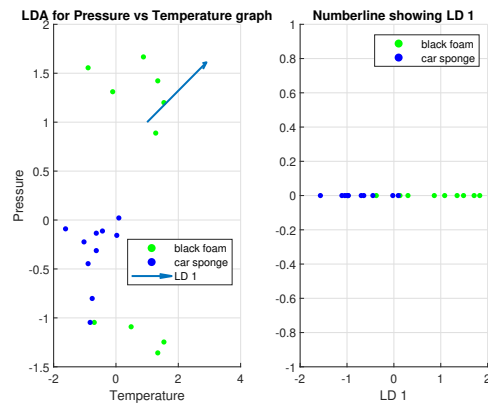


Figure 11: 2D scatter plot of Pressure vs Temperature for black foam and car sponge along with the dimension reduced data.

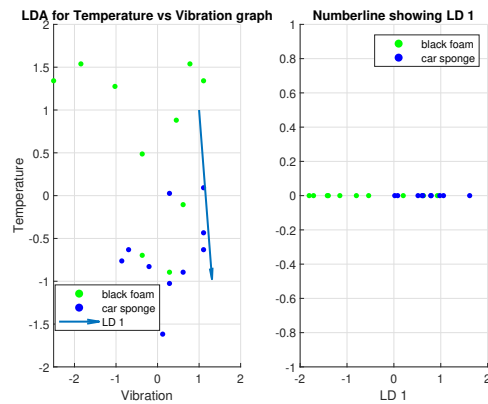


Figure 12: 2D scatter plot of Temperature vs Vibration for black foam and car sponge along with the dimension reduced data.

Part 1b

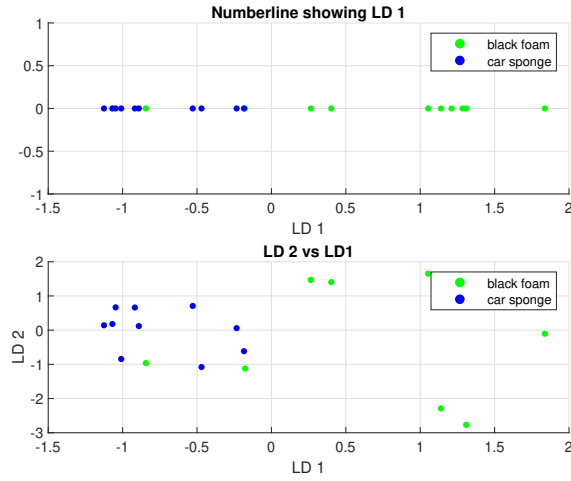


Figure 13: Data projected onto the main linear determinant (top graph) and the top two linear determinants (bottom graph).

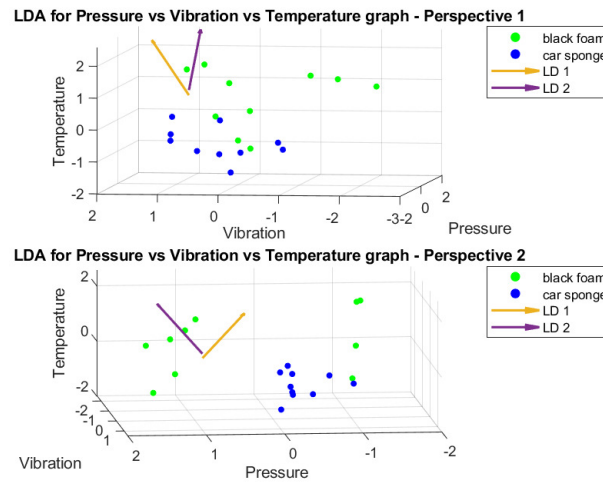


Figure 14: 3D scatter plot of the PVT data for black foam and car sponge along with the first 2 linear determinant lines.

Part 1d

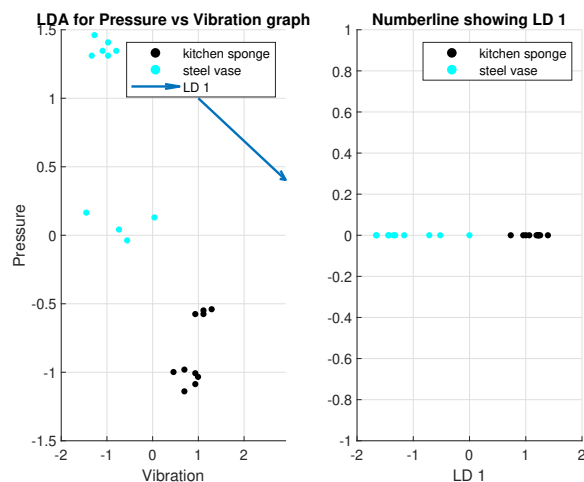


Figure 15: 2D scatter plot of Pressure vs Vibration for kitchen sponge and steel vase along with the dimension reduced data.

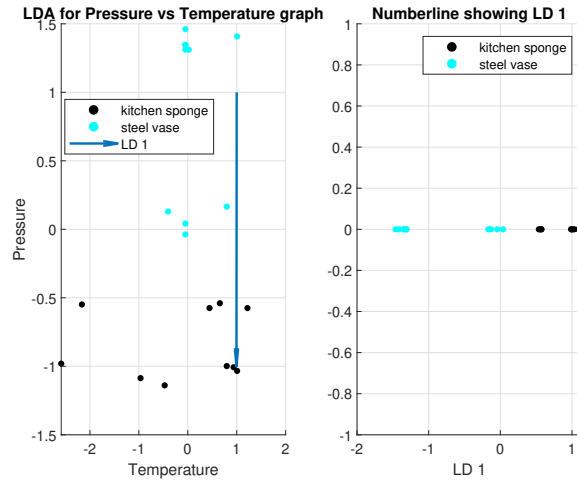


Figure 16: 2D scatter plot of Pressure vs Temperature for kitchen sponge and steel vase along with the dimension reduced data.

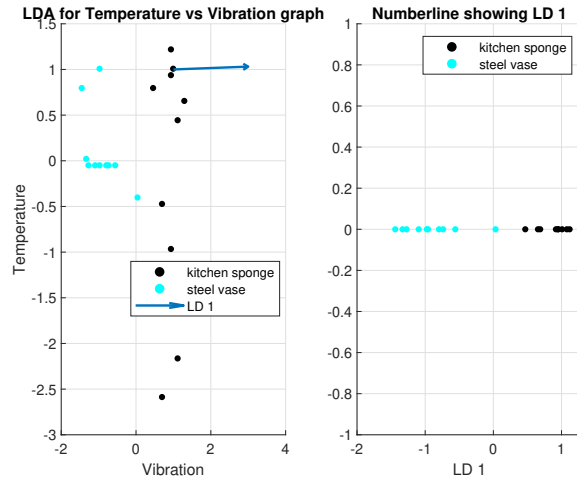


Figure 17: 2D scatter plot of Temperature vs Vibration for kitchen sponge and steel vase along with the dimension reduced data.

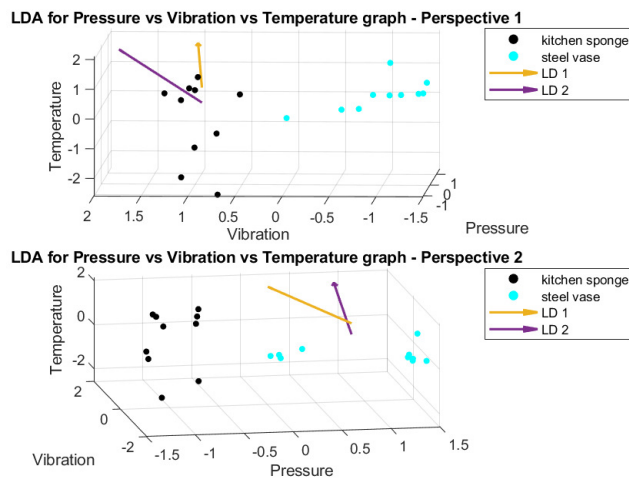


Figure 18: 3D scatter plot of the PVT data for kitchen sponge and steel vase.

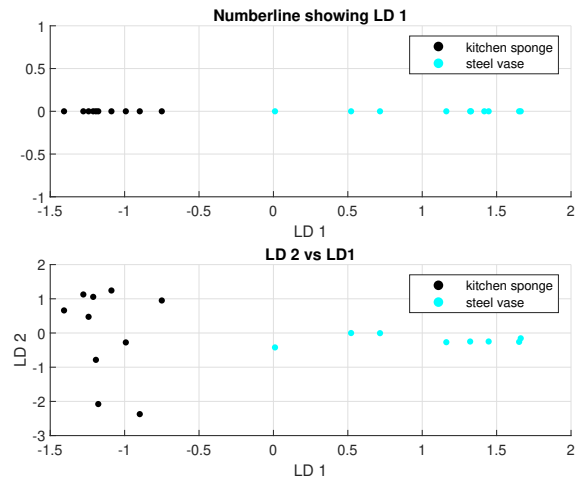


Figure 19: Data projected onto the main linear determinant (top graph) and the top two linear determinants (bottom graph).

Appendix D

Run section_d.m to obtain the images below.

Part 1a

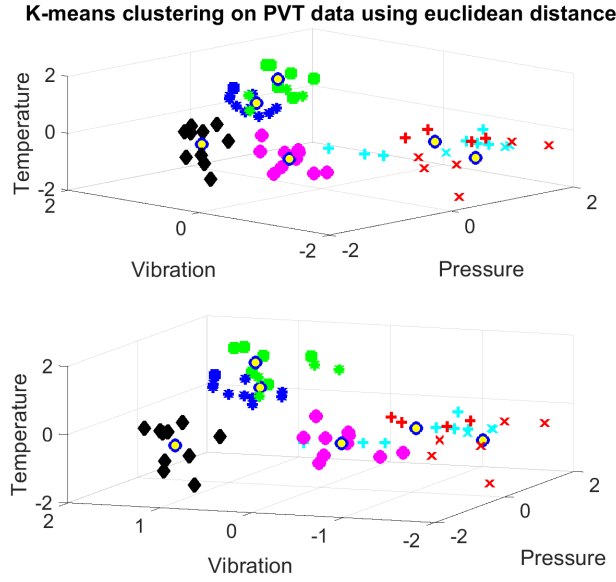


Figure 20: K-means output for PVT data using Euclidean distance. Colour scheme refers to objects as in previous sections. Clusters 1 to 6 are assigned a different shape ['o' , ' + ' , ' * ' , ' d ' , ' x ' , ' s '] respectively. Centroids are labelled as yellow points with blue edge.

Part 1c Correlation distance is defined one minus the sample correlation between points (treated as sequences of values). Each centroid is the component-wise mean of the points in that cluster, after centering and normalizing those points to zero mean and unit standard deviation [2].

$$d(x, c) = 1 - \frac{(x - \vec{x})(c - \vec{c})}{\sqrt{(x - \vec{x})(x - \vec{x})'} \sqrt{(c - \vec{c})(c - \vec{c})'}} \quad (4)$$

where x is an observation (that is, a row of X) and c is a centroid (a row vector). $\vec{1}_p$ is a row vector of p ones:

$$\vec{x} = \frac{1}{p} \left(\sum_{j=1}^p x_j \right) \vec{1}_p \quad (5)$$

$$\vec{c} = \frac{1}{p} \left(\sum_{j=1}^p c_j \right) \vec{1}_p \quad (6)$$

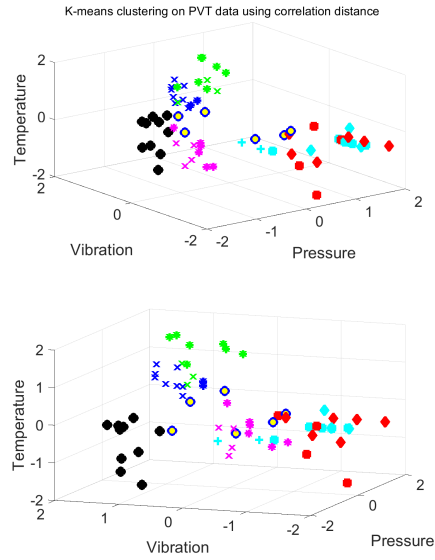


Figure 21: K-means output for PVT data using correlation distance. Colour scheme refers to objects as in previous sections. Clusters 1 to 6 are assigned a different shape ['o' , '+' , '*' , 'd' , 'x' , 's'] respectively. Centroids are labelled as yellow points with blue edge.

Part 2a

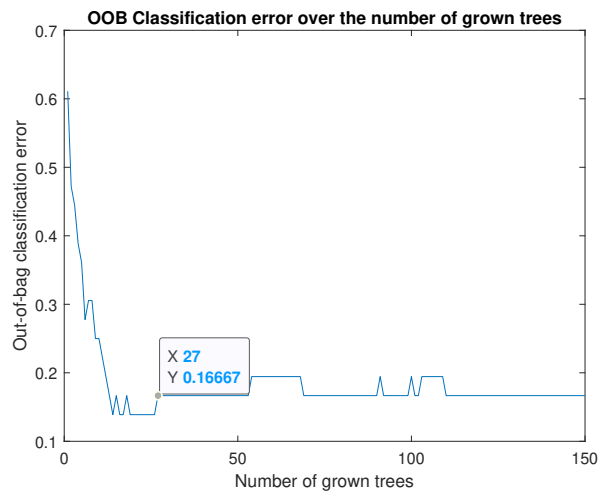


Figure 22: The Out-Of-Box Classification Error with 150 bags. The OOB error plateaus at 0.17 at around 30 bags/trees

Part 2b

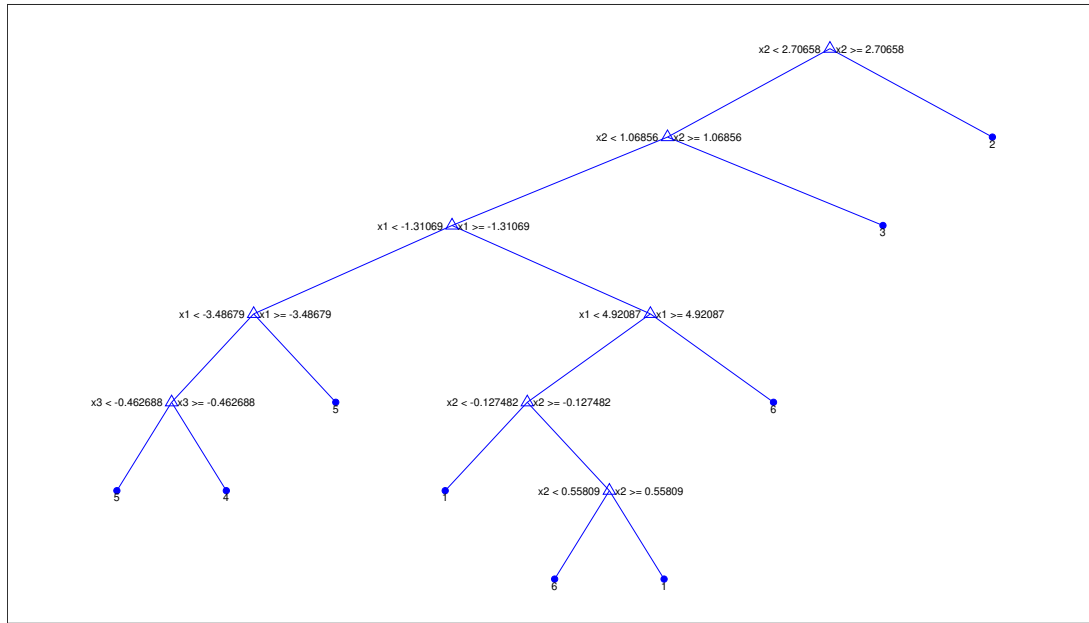


Figure 23: Visualization of Decision Tree 1 out of 30 trees

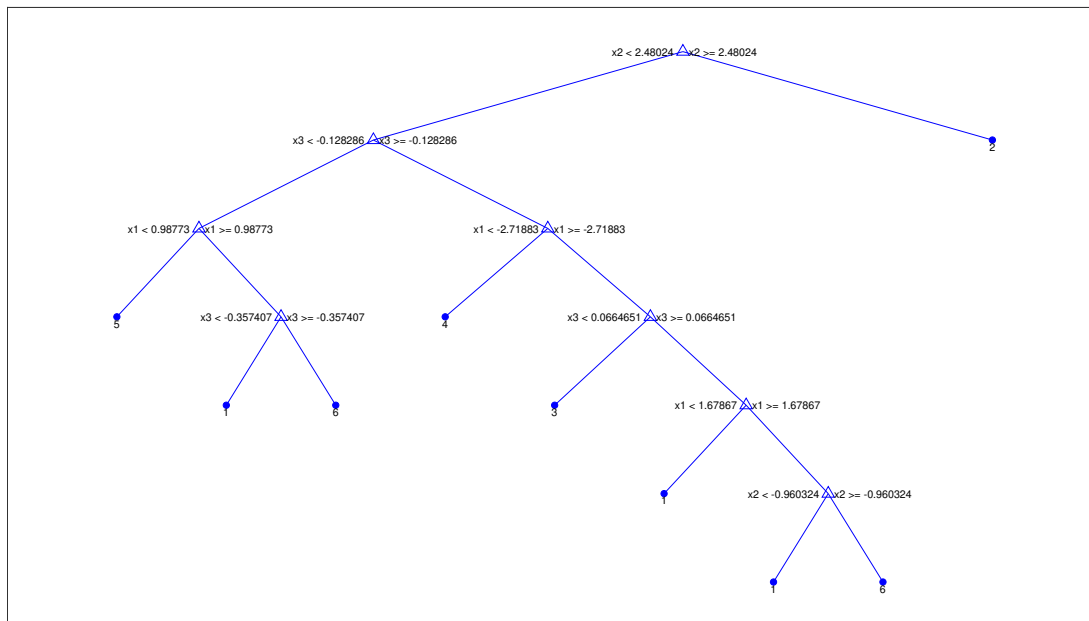


Figure 24: Visualization of Decision Tree 2 out of 30 trees

Part 2c

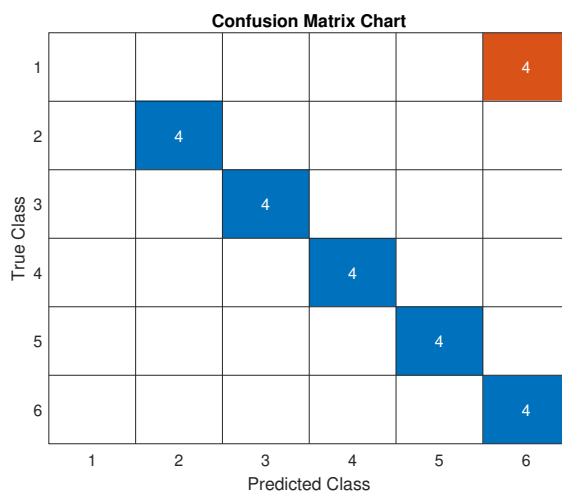


Figure 25: Confusion matrix - the main errors seem to occur when classifying acrylic data.

Part 2d

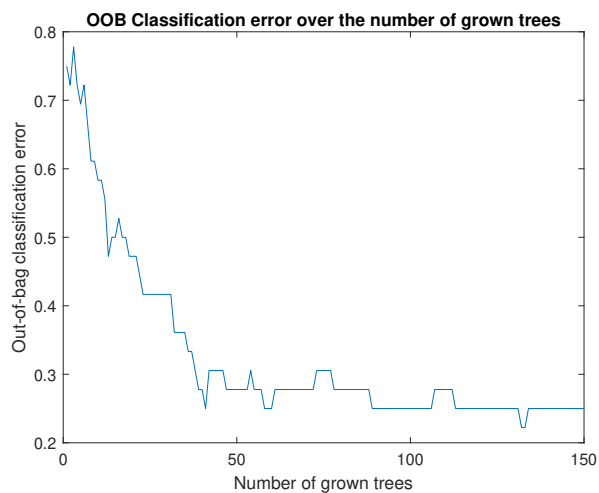


Figure 26: The plateau of the OOB Error occurs at around 50 bags when using 19 PCA axes, which is greater than the 30 bags gotten when using 3 PCA axes.